directly down dip. In the model, slip is imposed on this fault at a rate equal to the slip deficit accumulating on the plate interface. This slip, being a deficit, is in the opposite sense (that is, normal slip as opposed to thrust) to that occurring elsewhere on the plate interface. The surface deformation rates produced in the model are taken to represent the interseismic deformation rates observed on the overthrust plate (*14*).

The model fault for the Cascadia subduction zone off the Washington coast is specified as follows: The plate convergence rate is about 40 mm/year N68°E (*11*), and the fault dips 10° N68°E from the deformation front at the base of the continental slope (Fig. 1) at a depth of 2.5 km below sea level (*15*). Because the brittle-ductile transition on the fault occurs at a depth of about 20 km (*4*), the locked segment can extend only about 100 km down dip from the sea-floor trace at the deformation front. The slip deficit on this locked segment is equal to the plate convergence rate, 40 mm/year. Down dip from the locked segment is a transitional segment over which the slip deficit decreases from the full rate of 40 mm/year to zero. This transitional segment is a consequence of the elastic constraints limiting slip in the neighborhood of a pinned region (*16*). The transitional segment was arbitrarily assigned a 75-km down-dip dimension. We considered two arbitrary slip-deficit distributions (Fig. 3a) for the transitional segment of the plate interface, one in which the slip rate decreased linearly with down-dip distance and the other in which the decrease was proportional to the square root of that distance. The slip deficit was zero beyond 175 km down dip from the sea-floor trace (that is, at depths greater than 33 km). Finally, we assume that deformation is uniform in the direction of fault strike. The deformation rates predicted by the two different slip-deficit distributions (Fig. 3) assigned to the transitional segment of the plate interface are not significantly different at the level of observational precision.

The proposed model explains most of the observations relevant to the character of subduction at the Cascadia zone. The observed surface deformation rates (−0.089 ± 0.028 μstrain/year N68°E extension at the Olympic network, and uplift rates from Table 1) are in rough agreement with the rates predicted by the model (Fig. 3, b and c). Moreover, the shallow extent (maximum depth, 20 km) of the locked segment of the plate interface is consistent with the thermal constraints (*4*). The location of the locked segment beneath the continental slope and shelf implies that thrust events should occur offshore, where they are difficult to locate and identify, not beneath the Olympic Peninsula. Finally, rupture of the locked segment will produce the coastal coseismic subsidence inferred from the geologic record (*9*).

REFERENCES AND NOTES

1. G. C. Rogers, *Nature* **332**, 17 (1988); T. H. Heaton, *ibid.* **343**, 511 (1990).
2. J. J. Taber and S. W. Smith, *Bull. Seismol. Soc. Am.* **75**, 237 (1985).
3. R. S. Crosson, *ibid.* **62**, 1133 (1972); C. S. Weaver and S. W. Smith, *J. Geophys. Res.* **88**, 10371 (1983); M. L. Zoback, *U.S. Geol. Surv. Open-File Rep. 90-334* (1990), p. 537.
4. E. E. Davis, R. D. Hyndman, H. Villinger, *J. Geophys. Res.* **95**, 8869 (1990).
5. D. E. Byrne, D. M. Davis, L. R. Sykes, *Tectonics* **7**, 833 (1988).
6. T. H. Heaton and S. H. Hartzell, *Science* **236**, 162 (1987).
7. J. Adams, *Tectonics* **9**, 569 (1990).
8. B. F. Atwater, *Science* **236**, 942 (1987).
9. J. C. Savage, M. Lisowski, W. H. Prescott, *J. Geophys. Res.* **86**, 4929 (1981); M. Lisowski, W. H. Prescott, H. Dragert, *Seismol. Res. Lett.* **60**, 1 (1989).
10. J. C. Savage and W. H. Prescott, *J. Geophys. Res.* **78**, 6001 (1973).
11. C. DeMets, R. G. Gordon, D. F. Argus, S. Stein, *Geophys. J. Int.* **101**, 425 (1990).
12. S. D. Hicks, *J. Geophys. Res.* **83**, 1377 (1978).
13. W. R. Peltier and A. M. Tushingham, *Science* **244**, 806 (1989); A. M. Tushingham and W. R. Peltier, *J. Geophys. Res.*, in press.
14. J. C. Savage, *J. Geophys. Res.* **88**, 4984 (1983).
15. J. J. Taber and B. T. R. Lewis, *Bull. Seismol. Soc. Am.* **76**, 1011 (1986).
16. J. Weertmann, *ibid.* **54**, 1035 (1964).

17. We thank the Superintendent of Olympic National Park for permitting surveys within the park and R. Weldon for a constructive review of the manuscript.

7 November 1990; accepted 7 February 1991

Approaches for Optimizing the First Electronic Hyperpolarizability of Conjugated Organic Molecules

S. R. Marder, D. N. Beratan, L.-T. Cheng

A two-state, four-orbital, independent electron analysis of the first optical molecular hyperpolarizability, β, leads to the prediction that |β| maximizes at a combination of donor and acceptor strengths for a given conjugated bridge. Molecular design strategies that focus on the energetic manipulations of the bridge states are proposed for the optimization of β. The limitations of molecular classes based on common bridge structures are highlighted and more promising candidates are described. Experimental results supporting the validity of this approach are presented.

Second-order nonlinear optical properties, which are exploited in telecommunications, data storage, and information processing applications, arise in molecules that lack a center of symmetry (*1–4*). Such materials can be used to double the frequency of laser light or can be used in electrooptic switches, for example. Conjugated organic molecules with electron donating and accepting moieties can exhibit large electronic second-order nonlinearities (or first hyperpolarizabilities, β). In general, β increases with increasing donor and acceptor strength [related to the ionization potentials of the filled donor and empty acceptor orbitals or the coulomb energies of independent electron theory (*5*)] and with increasing separation so long as there is strong electronic coupling through the conjugated bridge.

The full perturbation theory expression for β has the form of a sum of contributions from all electronic states. However, for many donor-acceptor–substituted organics, such as 4-nitroaniline, a two-state approximation for β is adequate because the charge transfer (CT) excited-state term dominates the perturbation sum. The two-state expression for the dominant nonresonant component of the β tensor is proportional to:

$$(\mu_{ee} - \mu_{gg}) \frac{\mu_{ge}^{2}}{E_{ge}^{2}} \qquad (2)$$

where g is the index of the ground state, e is the index of the CT excited state, and μ is the dipole matrix element between the two subscripted states (*6*). For many organic molecules, the two-state expression accounts reasonably well for the experimental β values obtained by electric field–induced second harmonic generation (EFISH) measurements done in solution with a dc field (*7, 8*). Such experiments measure the vector projection of the hyperpolarizability tensor (β) along the molecular dipole (μ) direction. Although reservations exist for the general adequacy of the two-state approximation in extended molecules, it does capture the qualitative spectroscopic dependences of β for molecules with strong CT transitions. Simple molecular orbital considerations and the two-state approximation for β have been used to predict that a

---

S. R. Marder and D. N. Beratan, Jet Propulsion Laboratory, California Institute of Technology, Pasadena, CA 91109, and The Beckman Institute, California Institute of Technology, Pasadena, CA 91125.
L.-T. Cheng, E. I. DuPont de Nemours and Company, Inc., Wilmington, DE 19880–0238.

specific combination of donor and acceptor strengths for a given separation and bridge structure maximizes $|\beta|$ (9). In this report we reexamine the variations of spectroscopic and polarization parameters relevant in the two-state model for β with a series of four-orbital independent electron calculations. We propose a molecular design strategy that should enable the optimization of β for molecules with a given number of intervening bonds through a judicious choice of the bridge structure. We also present experimental results in support of our strategy.

Manipulation of the chemical properties of a chromophore can substantially alter the first hyperpolarizability, and these changes can be understood from Eq. 1. The terms in this equation are (i) the change in dipole moment between the two states, (ii) the square of the transition matrix element of the transition (proportional to the oscillator strength), and (iii) the inverse square of the transition energy. Since the individual terms each have their own characteristic maxima as a function of the molecular structure, maximizing the product of these factors requires compromise in the molecular design. Specifically, changing the electron donor and acceptor strength for a given conjugated bridge, or changing the nature of the bridge itself, varies these three factors substantially. In order to demonstrate the interrelation among $\mu_{ee} - \mu_{gg}$, μ_{ge}^2, the energy of the CT transition, and the dominant component of β, we performed a series of simple independent electron molecular orbital calculations on a four-orbital model system consisting of donor, acceptor, and bridge (5, 9). The coulomb energy difference between the donor (α_D) and the acceptor (α_A) was varied in 100 uniform increments from zero to $3|t|$ [where t is the exchange matrix element between the bridge orbitals and $2|t|$ is the energy gap between the highest occupied molecular orbital (HOMO) and the lowest unoccupied molecular orbital (LUMO) of the unsubstituted bridge]. Molecular orbitals were calculated for each value of $(\alpha_A - \alpha_D)/|t|$, as were $\mu_{ee} - \mu_{gg}$, μ_{ge}^2, and the energy difference between the HOMO and LUMO, so that β could be calculated with Eq. 1 (Fig. 1).

Several qualitative features emerge from this four-orbital analysis and the two-level model for β in bridged donor-acceptor molecules (9). In Fig. 1, small $(\alpha_A - \alpha_D)/|t|$ values represent strong mixing of donor and acceptor orbitals through the bridge whereas large $(\alpha_A - \alpha_D)/|t|$ values represent the decoupling of these orbitals from the bridge. When $(\alpha_A - \alpha_D)/|t| = 0$, the π electrons are symmetrically distributed in both the HOMO and LUMO, a condition in which both μ_{ge}^2 and $1/E_{ge}^2$ are maximized but the change in dipole moment, $\mu_{ee} - \mu_{gg}$, is zero. This corresponds to the case of a symmetrical cyanine chromophore (10) with a symmetric π-electron population or to the case of a neutral chromophore substituted with strong donors and acceptors such that the π-electron density is equally shared between the donor and acceptor. Thus, for neutral asymmetric molecules, large but equal ground- and excited-state dipole moments are expected. With increasing $(\alpha_A - \alpha_D)/|t|$, the HOMO takes on added acceptor and reduced donor character while the LUMO does the opposite. Thus, the π-electron distribution becomes increasingly asymmetric, resulting in reduced μ_{ge}^2 and $1/E_{ge}^2$ but increased $\mu_{ee} - \mu_{gg}$. This situation corresponds to the case of a somewhat unsymmetrical cyanine dye or of a chromophore with donor and acceptor substituents of moderate strength. For large $(\alpha_A - \alpha_D)/|t|$, the bridge-mediated donor-acceptor orbital mixing decreases and the HOMO and LUMO are largely bridge orbital in character. This decoupling leads to a further reduction of μ_{ge}^2 and $1/E_{ge}^2$ as well as a vanishing $\mu_{ee} - \mu_{gg}$, since the symmetrical bridge orbitals are largely unperturbed by the donor and acceptor. This corresponds to the case of a chromophore with very weak donor and acceptor groups. The optical transition in the ultraviolet (UV)-visible spectrum with most of the oscillator strength in such a molecule would be dominantly π-π^* in nature, with little CT character. Since β_{xxx} (the component of β along the CT axis) is the product of these three peaked functions according to Eq. 1, it also has a maximum that is on the low $(\alpha_A - \alpha_D)/|t|$ side of the $\mu_{ee} - \mu_{gg}$ peak. This result suggests that β_{xxx} is not maximized when the two states have the largest degree of charge transfer.

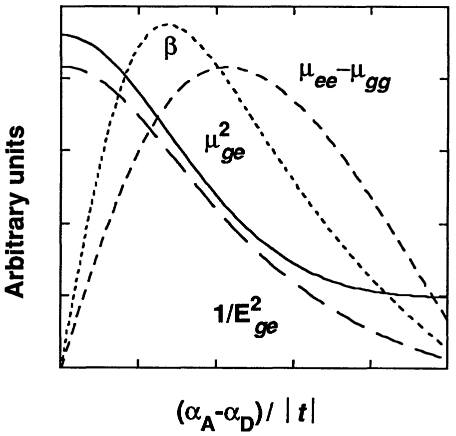

Fig. 1. The dependence of $\mu_{ee} - \mu_{gg}$, μ_{ge}^2, $1/E_{ge}^2$, and β on $(\alpha_A - \alpha_D)/|t|$ derived from molecular orbital calculations on a four-orbital system consisting of a donor, an acceptor, and two bridge orbitals is shown. The atoms are fixed at positions -2, -1, 1, and 2. Coupling between the bridge atoms is t and coupling between the bridge and end atoms is $0.8t$. The values of α_D and α_A were set equal to $-0.5|t|$ on the left edge of the plot and varied to $1.0|t|$ and $-2.0|t|$ on the right edge of the plot by increasing α_A and decreasing α_D symmetrically about $-0.5|t|$. Physically, this corresponds to strong donors and acceptors on the left and weak donors and acceptors on the right.

From a chemical design perspective, it is useful to discuss the wave functions of the ground and excited states in terms of a linear combination of the two limiting CT resonance structures. In this simple model, the relative energies of the two limiting resonance structures of a donor-acceptor molecule are influenced by two factors. First, a coulombic factor can be positive, negative, or zero depending on whether charges are separated, brought closer, or simply shifted, respectively. The second factor, a resonance energy, depends on the aromaticity of the π-electron system in the two limiting forms. The two resonance structures contribute equally to the ground and excited states when the coulombic and resonance factors balance, corresponding to a small value of $(\alpha_A - \alpha_D)/|t|$ in our independent electron calculations. When this relative energy difference increases, the ground and excited states become dominated by single resonance forms corresponding to increasing $(\alpha_A - \alpha_D)/|t|$. When the energy difference is very large, contributions from both resonance structures to the ground and excited state are expected to be small since the frontier orbitals will have little donor and acceptor orbital character, corresponding to the orbital decoupling at large $(\alpha_A - \alpha_D)/|t|$.

Many of the conjugated donor-acceptor systems that have been explored for second-order nonlinear optics fall into the categories of substituted benzenes, biphenyls, stilbenes, tolanes, and chalcones. Experimental β values were found to increase with increasing donor and acceptor strength. Indeed, one of the challenges identified for achieving large β in these molecules has been the search for stronger donors and acceptors, that is, reducing $(\alpha_A - \alpha_D)/|t|$ in our model. However, all of these molecules have dominantly aromatic ground states. The corresponding electron transfer states have predominantly quinonal ring structures. Electronic polarization, arising from an applied electric field, results in a perturbed ground-state wave function with increased quinonal character and decreased resonance stabilization energy (Fig. 2A). Thus, the aromatic nature of the ground state should impede electronic polarization in an applied field. As a result, the effective donor and acceptor strength of a given pair connected by an aromatic bridge would be lower than when they are attached to a degenerate π-electron system, which has equivalent res-

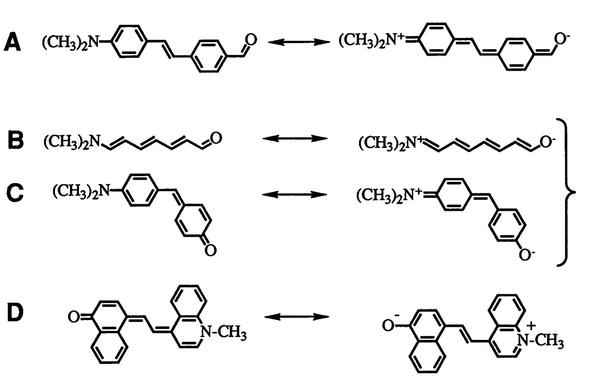

Fig. 2. Limiting resonance forms for molecules with (**A**) an aromatic ground state where resonance energy is lost in the CT state, (**B**) polyene, (**C**) aromatic-quinonal ground state where resonance energy does not change in the CT state, and (**D**) quinonal ground state where resonance energy is gained in the CT state.

onance energies (where terminal p-orbital energy difference effects are ignored) in both the neutral and polarized forms (Fig. 2, B and C). Such a bridge would neither assist nor impede charge transfer. Compounds with somewhat quinonal ground states and aromatic excited states can be synthesized and tend to assist charge polarization (Fig. 2D) (*11*).

Based on the energetic considerations detailed above, we suggest that the choice of an aromatic ground state is the predominant factor that has limited the magnitude of β for a given chain length. Molecules that have degenerate ground states in both CT configurations, such as those that have equal aromatic and quinonal character in the ground state, should not lose aromaticity upon charge transfer. This would greatly diminish the effective $(\alpha_A - \alpha_D)/|t|$ and may allow one to optimize β. We therefore sought to examine molecules with π systems such as that in Fig. 2C. In the ground state, one ring of this π system is aromatic, and the other ring is quinonal. In the charge-separated state, the aromatic-quinonal nature of each ring is reversed, preserving the π-electron degeneracy. Similar reasoning has been used to design low band gap polymers; for these materials enhancements in the linear polarizability due to quinonal character have been described (*12*).

Dimethylaminoindoaniline (DIA) is a commercially available dye with the electronic degeneracy outlined above. Steric interactions between the ortho hydrogens of the rings preclude them from being coplanar, undoubtedly resulting in a decreased oscillator strength and polarizability compared to an equivalent system "forced" to be coplanar. Nevertheless, this compound is a logical starting point to test our hypothesis. The EFISH measurements (*13*) on this compound in chloroform at 1.907 μm yielded a β of 190 × 10^{-30} esu (Table 1). The low absorption edge leads to a dispersive contribution. Correcting for dispersion with the two-level model (*7*, *14*) gives the zero frequency value $\beta_0 = 106 \times 10^{-30}$ esu. In contrast, for dimethylaminonitrostilbene (DANS), $\beta = 73 \times 10^{-30}$ esu and $\beta_0 = 55 \times 10^{-30}$ esu. Thus, although DIA is bent (resulting in a substantially shorter charge separation axis compared to a more linear molecule like DANS), is two atoms shorter than DANS, and lacks coplanar rings, β is roughly a factor of 3 greater and β_0 is almost a factor of 2 greater.

We hypothesized that breaking the degeneracy of the π system (keeping the overall length of the molecule constant) would in general result in a lower hyperpolarizability. We tested this hypothesis by examining indophenol blue (IPB). This dye is sold commercially as a mixture of isomers that can be readily separated by chromatography. We predicted that both IPB 1 and 2 would have lower β values than DIA since one of the double bonds of the "quinone" is already involved in aromatic bonding. Thus the gain of aromaticity in the charge-separated forms of IPB 1 and 2 would be expected to be less than in the case of DIA. The measured β values of 79 × 10^{-30} esu for IPB 1 and 91 × 10^{-30} esu for IPB 2 are consistent with the hypothesis. Another interesting comparison is to 5-(4-*N*, *N*-dimethylamino)phenylpentadienal (DPPD), which is structurally similar to DIA but lacks the double bond critical for the degeneracy of the π system. The β value for this compound is 52 × 10^{-30} esu. These results are strongly suggestive that the enhanced nonlinearity of DIA is largely due to the degenerate π system.

One prediction of our model is that the hyperpolarizability of DIA should be sensitive to the amount of neutral and CT character in the ground state. Since DIA has a degenerate π system, the effective difference in energy between the neutral and CT forms would be dictated by coulombic factors. The absorption maximum (λ_{max}) of DIA shifts to longer wavelength in more polar solvents (λ_{max}, 585 nm, in acetone; λ_{max}, 679 nm, in water) (*15*). Polar solvents that can stabilize charge separation would make the two resonance forms more energetically equivalent. Therefore, the ground state of DIA in a nonpolar solvent favors the neutral bond-alternated form, whereas in polar solvents the CT form would contribute more equally and lead to a polar, less bond-alternate (more cyanine-like) ground state (*15*). In terms of the plots shown in Fig. 1, $(\alpha_A - \alpha_D)/|t|$ decreases with decreasing bond alternation, which is reflected experimentally by the longer λ_{max} of DIA in more polar solvents. Therefore, we expected β to increase with decreasing $(\alpha_A - \alpha_D)/|t|$ (increasing λ_{max}) and then possibly decrease if $(\alpha_A - \alpha_D)/|t|$ became sufficiently small (as indicated by even longer λ_{max} in very polar solvents, Fig. 1) (*16*). Accordingly, EFISH measurements of DIA were performed in a variety of solvents ranging in polarity from cyclohexane to *N*-methyl-2-pyrrolidinone (NMP) (*17*). As

Table 1. Summary of structures, abbreviations for structures, β values, β_0 values, and λ_{max} values (measured in chloroform) for compounds discussed in this report. Details of the EFISH experiment are discussed elsewhere (*13*).

Chemical structure (abbreviation)		β (10^{-30}esu)	β_0 (10^{-30}esu)	λ_{max} (nm)
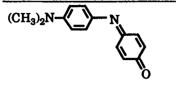	(DIA)	190	106	590
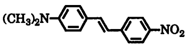	(DANS)	73	55	430
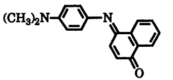	(IPB 1)	79	43	580
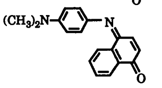	(IPB 2)	91	48	610
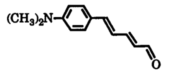	(DPPD)	52	40	412

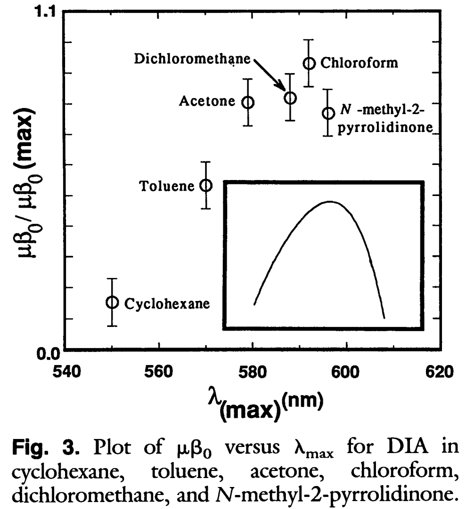

Fig. 3. Plot of $\mu\beta_0$ versus λ_{max} for DIA in cyclohexane, toluene, acetone, chloroform, dichloromethane, and *N*-methyl-2-pyrrolidinone. Although the large dielectric constant of the very polar solvents precluded independent measurement of the ground-state dipole moment, it is expected that the dipole moment of DIA in NMP would be greater than that in the other solvents, further decreasing its relative value of β. The insert at the lower right shows a plot of $\mu\beta_0$ versus $1/E_{ge}$ (proportional to λ_{max}) from the four-orbital calculation for comparison. The precision for the reported β values is ±10% of the measured value (*19*).

can be seen in Fig. 3, $\mu\beta_0$ increased with increasing λ_{max} and reached a maximum value and possibly decreased as λ_{max} became sufficiently long (*18*).

Brooker has synthesized molecules with ground states that are neutral and aromatic, zwitterionic and aromatic, as well as molecules that have weak quinonal contributions to the ground state (*10*). He has shown that one can effectively tune from bond-alternate neutral structures through polar non–bond-alternate structures to extremely polar bond-alternate structures by making appropriate choices of the aromatic-quinonal character of the end groups. Introduction of too much quinonal character in the neutral form of the molecule may not be desirable, since it could result in a very polar, aromatic ground state. Molecules like these generally have negative β since the excited-state dipole moment is usually less than the ground-state dipole moment (*11, 16*). Thus, it is important to realize that the key to successful implementation of our strategy is to have the correct energetic balance between the neutral and CT states and not to simply stabilize the CT state.

The theoretical and experimental results reported here suggest that by the correct choice of the degree of aromatic-quinonal character in the ground-state wave function it should be possible to strike the optimal compromise for relative energetics of the neutral and CT resonance forms, in effect tuning the $(\alpha_A - \alpha_D)/|t|$ to optimize β. Brooker has found that, for cyanine-like molecules, increased electronic asymmetry leads to decreased μ_{ge}^2 and λ_{max}, in qualitative agreement with the results of Fig. 1. We suggest that these observations form the basis of a procedure to maximize β for a given conjugation length.

REFERENCES AND NOTES

1. D. J. Williams, *Angew. Chem. Int. Ed. Engl.* **23**, 690 (1984).
2. ———, Ed., *Nonlinear Optical Properties of Organic and Polymeric Materials*, no. 233 of the *ACS Symposium Series* (American Chemical Society, Washington, DC, 1983).
3. S. R. Marder, J. E. Sohn, G. D. Stucky, Eds., *Materials for Nonlinear Optics: Chemical Perspectives*, no. 455 of the *ACS Symposium Series* (American Chemical Society, Washington, DC, 1991).
4. D. S. Chemla and J. Zyss, Eds., *Nonlinear Optical Properties of Organic Molecules and Crystals* (Academic Press, Orlando, FL, 1987), vols. 1 and 2.
5. C. J. Ballhausen and H. B. Gray, *Molecular Orbital Theory* (Benjamin, New York, 1964).
6. J. F. Ward, *Rev. Mod. Phys.* **37**, 1 (1965); B. J. Orr and J. F. Ward, *Mol. Phys.* **20**, 513 (1971).
7. J. L. Oudar and D. S. Chemla, *J. Chem. Phys.* **66**, 2664 (1977); B. F. Levine and C. G. Bethea, *ibid.*, p. 1070; S. J. Lalama and A. F. Garito, *Phys. Rev. A* **20**, 1179 (1979).
8. J. L. Oudar and H. Le Person, *Opt. Commun.* **15**, 258 (1975); B. F. Levine and C. G. Bethea, *Appl. Phys. Lett.* **24**, 445 (1974); K. D. Singer and A. F. Garito, *J. Chem. Phys.* **75**, 3572 (1981).
9. M. M. Choy, S. Ciraci, R. L. Byer, *IEEE J. Quantum Electron.* **QE-11**, 40 (1975); D. J. Williams, *Adv. Chem. Ser.* **218**, 298 (1988); D. N. Beratan, in (*3*), pp. 89–102.
10. L. G. S. Brooker and R. H. Sprague, *J. Am. Chem. Soc.* **63**, 3203 (1941); L. G. S. Brooker *et al.*, *ibid.*, p. 3192; ———, G. H. Keyes, W. W. Williams, *ibid.* **64**, 199 (1942); L. G. S. Brooker and R. H. Sprague, *ibid.* **67**, 1869 (1945); L. G. S. Brooker, *Rev. Mod. Phys.* **14**, 275 (1942).
11. Quinonal structures have been studied previously and exhibit large negative values for β: A. F. Garito, K. D. Singer, C. C. Teng, in (*2*), pp. 1–26.; S. J. Lalama *et al.*, *Appl. Phys. Lett.* **39**, 940 (1981).
12. J. L. Bredas, *Synth. Met.* **17**, 115 (1987); ——— *et al.*, *ibid.* **28**, 533 (1989).
13. L.-T. Cheng *et al.*, *Proc. SPIE* **1147**, 61 (1989). The uncertainty in the reported β values is ±10% of the measured value.
14. K. D. Singer, J. E. Sohn, S. J. Lalama, *Appl. Phys. Lett.* **49**, 248 (1986).
15. L. G. S. Brooker and R. H. Sprague, *J. Am. Chem. Soc.* **63**, 3214 (1941).
16. The hyperpolarizability of a merocyanine dye measured in two solvents has been reported previously: B. F. Levine *et al.*, *J. Chem. Phys.* **68**, 5042 (1978).
17. M. J. Kamlet *et al.*, *J. Org. Chem.* **48**, 2877 (1983); M. J. Kamlet, J. L. M. Abboud, R. W. Taft, *Prog. Phys. Org. Chem.* **13**, 485 (1981), and references therein.
18. Since DIA is known to absorb at very long wavelengths in water, leading to nearly equal contributions from the neutral and CT resonance forms (*15*), the β value of DIA in water is expected to be much less than that in chloroform. Unfortunately, water cannot support the large dc fields used to orient the chromophores in the EFISH experiment, so it was not possible to perform measurements in this solvent.
19. A more complete discussion of error analysis is presented in L.-T. Cheng *et al.*, unpublished results.

20. The work in this paper was performed in part by the Center for Space Microelectronics Technology, Jet Propulsion Laboratory (JPL), California Institute of Technology, and was sponsored by the Strategic Defense Initative Organization, Innovative Science and Technology Office through an agreement with the National Aeronautics and Space Administration (NASA). Additional support for this work at JPL was provided by the Department of Energy's Catalysis/Biocatalysis Program, Advanced Industrial Concepts Division, through an agreement with NASA. We thank H. Jones for expert technical assistance and J. W. Perry, B. G. Tiemann, D. A. Dougherty, G. R. Meredith, and J. J. Hopfield for helpful discussions.

22 October 1990; accepted 17 January 1991

Reconciling the Magnitude of the Microscopic and Macroscopic Hydrophobic Effects

KIM A. SHARP, ANTHONY NICHOLLS, RICHARD F. FINE,
BARRY HONIG*

The magnitude of the hydrophobic effect, as measured from the surface area dependence of the solubilities of hydrocarbons in water, is generally thought to be about 25 calories per mole per square angstrom (cal mol^{-1} Å^{-2}). However, the surface tension at a hydrocarbon-water interface, which is a "macroscopic" measure of the hydrophobic effect, is ≈72 cal mol^{-1} Å^{-2}. In an attempt to reconcile these values, alkane solubility data have been reevaluated to account for solute-solvent size differences, leading to a revised "microscopic" hydrophobic effect of 47 cal mol^{-1} Å^{-2}. This value, when used in a simple geometric model for the curvature dependence of the hydrophobic effect, predicts a macroscopic alkane-water surface tension that is close to the macroscopic value.

HYDROPHOBICITY IS GENERALLY associated with the increases in free energy and heat capacity that are observed when nonpolar solutes are transferred from nonpolar solvents to water (*1, 2*). The observation that the free energy increase is primarily entropic in origin at lower temperatures but becomes increasingly enthalpic as the temperature is raised recently has led to questions about the precise origin of the effect (*3–5*). In this report we focus on the magnitude of the hydrophobic effect in the physiological temperature range. At these temperatures, the free energy change is primarily due to a decrease in entropy that arises from a poorly defined ordering of water molecules around the solute.

Hydrophobic free energies have been obtained from measurements of the solubility of hydrocarbons in water and from partition coefficients of various solutes between aqueous and nonpolar phases. The observed free energy changes have been correlated with accessible surface areas (*6*), and coefficients ranging from 16 to 31 cal mol^{-1} Å^{-2} have been reported (*7–10*). This variation is in part due to the use of different solvents, different measures of surface area, and different approaches to fitting the data.

In this report we focus primarily on aliphatic hydrocarbons because there is a great deal of experimental data available and because these molecules have negligible electrostatic and hydrogen-bonding contributions to solvation. The change in standard state chemical potential, $\Delta\mu^0$, on transfer of

---

K. A. Sharp, A. Nicholls, B. Honig, Department of Biochemistry and Molecular Biophysics, Columbia University, 630 West 168 Street, New York, NY 10032.
R. F. Fine, Biosym Technologies, Inc., San Diego, CA 92121.

*To whom correspondence should be addressed.